



Multi-scale quantification of leaching performance using X-ray tomography



Q. Lin^a, S.J. Neethling^{a,*}, L. Courtois^{b,c}, K.J. Dobson^{b,c}, P.D. Lee^{b,c}

^a Rio Tinto Centre for Advanced Mineral Recovery, Department of Earth Science and Engineering, Imperial College London, London SW7 2AZ, United Kingdom

^b Manchester X-ray Imaging Facility, School of Materials, University of Manchester, Oxford Rd., M13 9PL, United Kingdom

^c Research Complex at Harwell, Rutherford Appleton Laboratories, Harwell, Didcot, Oxfordshire OX11 0FA, United Kingdom

ARTICLE INFO

Article history:

Received 26 February 2016

Received in revised form 28 May 2016

Accepted 23 June 2016

Available online 25 June 2016

Keywords:

Heap leaching

Multi-scale

Micro-CT

Imaging

Leaching variability

ABSTRACT

The performance of heap leaching is dictated by a large number of processes acting at a wide range of length scales. One important scale is that of the individual particles, where the interaction between the rate kinetics at the surfaces of the individual mineral grains and the mass transport through the particle combine to give the overall apparent particle scale kinetics. It has been recognised for a long time that variability in the mineralogy, size and spatial distribution of the mineral grains within the particle are likely to have a large effect on the leach performance and its variability and thus, ultimately, the performance of the heap. In this paper a new method for quantifying this behaviour and its variability at scales from the particle through to the grain and down to the surface kinetics is presented. This method is based on the use of a series of XMT (also called micro-CT) images of a column taken at regular intervals over 168 days of leaching. The key development in the analysis of this data is an algorithm that has allowed every single one of the hundreds of thousands of mineral grains within the column to be individually tracked across all the time points as they undergo dissolution. This has allowed the dependency of the mineral grain leach rate on its size and position in the particle to be decoupled from one another. It also meant that the variability in the surface kinetics of the grains could be assessed, with mineralogical variability being the key source of this variability. We demonstrate that understanding and quantifying this underlying kinetic variability is important as it has a major impact on the time evolution of the average kinetics of the leaching.

© 2016 The Authors. Published by Elsevier B.V. This is an open access article under the CC BY license (<http://creativecommons.org/licenses/by/4.0/>).

1. Introduction

While metal production has kept pace with increased demand this has generally been achieved by exploiting deposits with more problematic mineralogies and ever lower ore grades. As the grades of ores decrease, heap leaching is becoming a more attractive alternative to conventional processing routes, such as flotation followed by smelting, as it does not require milling of the ore and the operating cost per unit of metal is thus less sensitive to grade. Approximately 20% to 30% of the world's copper and more than 12% of gold is produced by this technique (Bouffard and West-Sells, 2009; Jergensen, 1999; Kappes, 2005). The biggest disadvantages of heap leaching, though, are the long processing time and relatively low extraction efficiencies, especially for primary sulphides.

Research into heap leaching can be divided into a range of spatial scales involving different processes and sub-processes, including the

macro-scale (heap scale effects), meso-scale (groups of particles, typically investigated through column scale studies), individual ore particle scale and grain scale (Dixon and Petersen, 2003). At each scale, there are several different sub-processes and control parameters which can affect leach behaviour. In general, conditions and concentrations in the fluids around the ore particle, the mass (and heat) transport within the ore particle and surface reaction kinetics are the main factors which can affect the leach performance at the meso-scale and which determine the apparent leach kinetics. Most studies of heap leaching have either concentrated on the first or last of these factors, either using particle sizes representative of real heaps and studying the apparent kinetics as a function of the effluent and/or feed conditions (e.g. van Hille et al. (2010)) at column or larger scale, or have attempted to obtain the surface reaction kinetics by studying the dissolution of finely milled ore or pure mineral particles in stirred tank experiments (Córdoba et al., 2008; Hiroyoshi et al., 2001) at the grain scale. A lack of data on the transport processes within the ore particles makes it very hard to predict heap or even particle scale leach performance based directly on the surface reaction kinetics, while only studying the behaviour based on the overall performance makes it hard to determine the dominant mechanisms at

* Corresponding author at: Department of Earth Science and Engineering, Royal School of Mines, Imperial College London, SW7 2BP, United Kingdom.
E-mail address: s.neethling@imperial.ac.uk (S.J. Neethling).

work and how these vary spatially, temporally and with operating conditions.

The aim of this paper is not to attempt to mimic all the variability encountered in a real heap or to measure the impact of variability in the fluid conditions around the particles, but to rather examine the leach behaviour and its variability at the scale of the individual particles and the mineral grains within them. An experimental system consisting of multiple small columns was chosen, as this would ensure that all the particles within them would experience similar leach conditions. Small columns have the added advantage of being able to be repeatedly scanned at high resolution.

The technology that allowed us to study the grain scale leach behaviour is X-ray micro-computed tomography (XMT, also termed μ CT) coupled to advanced image analysis algorithms. The advantage of XMT is its ability to image the internal structure of materials, including geological samples (Ghorbani et al., 2011b, 2013; Ketcham and Carlson, 2001) in a non-destructive manner. XMT produces images based on differences in X-ray attenuation, which, in turn, depends on the electron density and hence a combination of the density and atomic mass of the materials. This means that within the copper ore used in this study the sulphide species can be readily distinguished from the mainly silicate gangue, though the various sulphide species have similar attenuations and are thus hard to distinguish from one another.

In this work XMT has allowed 3D images of the mineral grain distributions to be obtained within the same leaching particles at a succession of time points. In order to analyse this data we have developed advanced image quantification algorithms (Lin et al., 2015) that have allowed us to track the dissolution of many hundreds of thousands of individual mineral grains over the course of many months of leaching. The analysis of this data set is thus the main focus of this paper. It should be noted that due to the difficulty in distinguishing different sulphide phases this paper examines the dissolution of the sulphide grains rather than specifically the copper extraction. In later sections where the grain scale variability is quantified, much of this will therefore come from mineralogical variability.

2. Experimental methodology

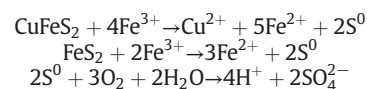
The leached sample consisted of copper sulphide ore particles from Kennecott with a size ranging between 8 and 11.2 mm. The ore composition was obtained using the Mineral Liberation Analyser (MLA) (see Table 1).

As this method is destructive, the composition is not that of the actual particles in the column, but rather that of similar particles.

The small scale column leaching experiments were carried out using an incubator with temperature control, which allows multiple columns to be run at the same time. The reason for using an incubator is because, despite the exothermic reactions, small columns lose too much heat to

be able to maintain the temperatures typically encountered within a heap. In these experiments the incubator was maintained at a temperature of 60 °C. Fig. 1 shows a schematic diagram of the experiment setup, a photograph showing a few of the columns loaded with ore particles and undergoing leaching, as well as the scanning regions for each column (blue). Glass columns with a 28 mm internal diameter and 190 mm height were used in the experiments. The resolution of the XMT images depends on the diameter of the sample being scanned. The diameter of the column used is thus the result of a compromise between the amount of sample being leached and the resolution of the 3D images produced.

The leach solution used in these experiments contained 5 g/L Fe^{3+} as iron sulphate, as well as 0.1 M H_2SO_4 to achieve a feed pH of approximately 1. The flow rate of this solution into the column was 160 $\mu\text{L}/\text{min}$, which is equivalent to approximately 16 $\text{L}/\text{m}^2/\text{h}$. The flow rate was controlled by a multi-channel peristaltic pump. The solution was not recycled. The ferric ions were added to the solution to act as the main leaching agent. This was done to mimic the effect of bacterial action, which in an actual heap would generate ferric ions mainly through a combination of the leaching of the pyrite and the oxidation of the ferrous ions in solution. While there is still some controversy as to the exact mechanisms involved, especially for chalcopyrite, the overall ferric leaching reactions for the chalcopyrite and pyrite are typically described as being as follows, with a subsequent reaction in which a portion of the elemental sulphur is converted to a sulphate (Habashi, 1999):



3. Image acquisition and processing methodology

The columns used in this study were scanned using a Nikon Metris Custom Bay with a 1 mm aluminium filter (to reduce beam hardening effects), 89 kV energy, 0.708 s exposure time and 2001 projections. The detector size was 2000×2000 pixels, which gave a linear resolution of approximately 17 μm . Three volumes (top, middle and bottom for each column) were scanned at each time point over the leaching period. Scanning was done by removing the entire column from the incubator and placing it within the scanner before replacing it within the incubator. This was done as rapidly as possible in order to minimise the disturbance to the column. As the leaching rate in the columns decreased with time, the interval between scans was increased. The scanning intervals are given in Table 2.

While the entire column was initially imaged, in subsequent scans the same three sub-volumes of the column were imaged (see Fig. 1). The reason for doing this was a combination of the most efficient use of the available equipment time, as well as the desire to minimise disruption of the feed and heating of the column. The total number of tracked whole ore particles¹ within these three sub-volumes was 26 for this column.

After scanning, the images needed to be reconstructed and relevant data quantified. The main image processing steps were as follows:

1. The reconstructed image had a $3 \times 3 \times 3$ median filter applied to reduce the noise level.
2. The rock phase was thresholded using the Otsu algorithm (Otsu, 1979). This algorithm was used as there are distinct peaks in the intensity histogram between the rock and the air phases.

¹ A whole ore particle means one where the entire ore particle appears in all the images. Ore particles were ignored when only part of the particles appeared in the scan.

Table 1

Main mineral species within ore sample used in experiments. Prevalence is reported as volume percentages as these are most relevant to micro-CT analysis, which also measures volume.

Mineral type	vol.%
Copper containing species	1.05
Chalcopyrite	0.58
Covellite	0.15
Cu oxides	0.03
Other Cu minerals	0.29
Pyrite	4.43
Gangue minerals	94.5
Quartz	51.4
Muscovite	39.9
Clays	1.0
Other gangue minerals	2.2

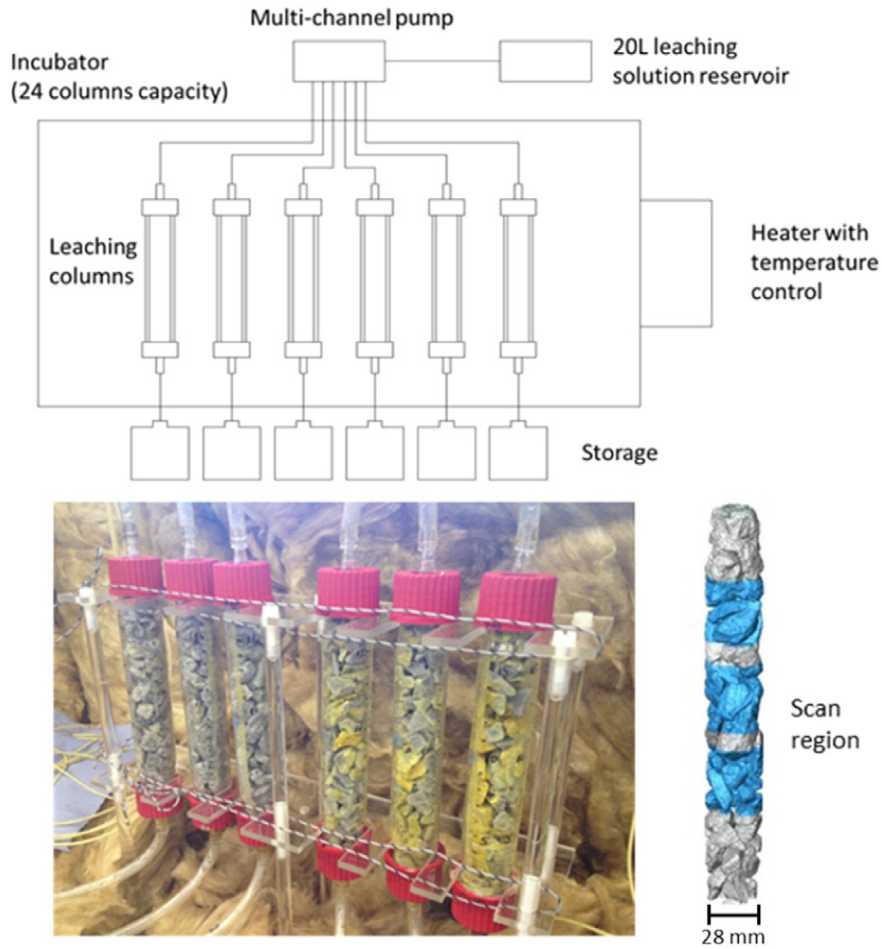


Fig. 1. Schematic diagram of small scale column leaching experiment and columns filled with ore particles and the scanning regions.

3. The connected ore particles were separated using a distance transformation based method with marker control to avoid over segmentation.
4. Each ore particle was then labelled and tracked over the leaching period using a centroid tracking algorithm (Blair and Dufresne, 2008). This was required both because the ore particles settle and rotate over the course of the leaching and because the orientation of the column varies slightly between scans.
5. After extracting the same ore particle from different scans, the initial ore particle was registered according to the later scan in order to have the same orientation at each time point. The extracted 4×4 transformation matrix is a key input into the grain tracking algorithm.
6. The mineral grain phase was then thresholded using the Maximum Entropy algorithm (Kapur et al., 1985). The reason for using this algorithm is that the relatively small quantity of sulphide in the ore means that it does not exhibit a distinct peak in the intensity histogram.
7. All the mineral grains in the scanned volume were then tracked individually using a new fast tracking method. A detailed description of the grain tracking methodology can be found in Lin et al. (2015). Fig. 2a) and b) show a slice through a particle before leaching and after 168 days of leaching in which all the grains have been correctly

matched to their corresponding grains in the earlier image despite some of the grains disappearing completely or splitting into multiple segments. Fig. 2c) shows the tracking of a single large grain over the course of the experiment.

4. Investigation of leach performance and variability

In this section the leach behaviour and its variability at different scales are investigated. The average sulphide dissolution for the entire column, the average sulphide dissolution for the three scanning regions and the sulphide dissolution for all the tracked ore particles can be measured from the image analysis (Fig. 3), each showing different levels of variability.

4.1. Leach performance and variability at the particle scale

The vertical leach variability is small, with no discernible trend in the extraction with height (Fig. 4d). This is due to the scale of the column and the narrowly sized ore particles. The horizontal leach variability can also be measured by considering the location of the ore particles, which is characterised by the distance between the centroid of each particle and the centre of the column (Fig. 5). As the column is very narrow (internal diameter of the column was 28 mm), the flow can spread

Table 2
XMT scanning intervals for the small scale leaching columns.

Scanning points (end of leaching day)												
0	1	5	11	16	23	33	43	53	83	118	136	168

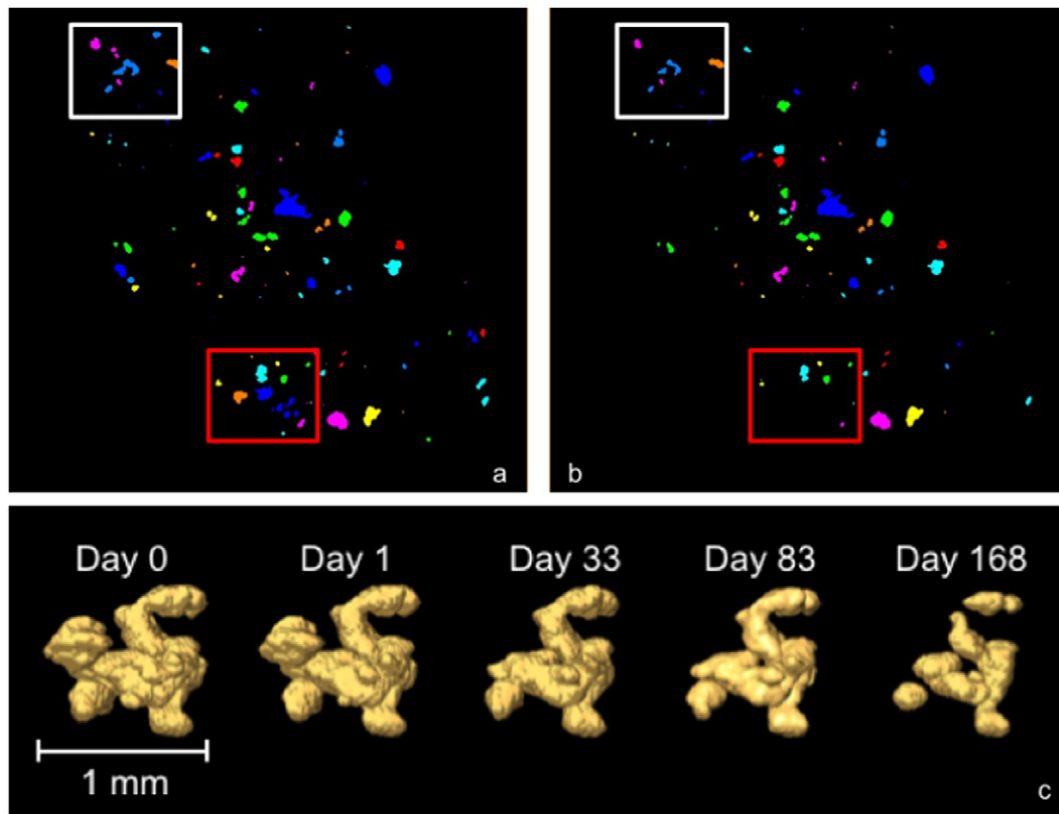


Fig. 2. Examples showing mineral grain tracking. a–b) An example slice of mineral grains within an ore particle after leaching. Different colours indicate individual mineral grains. c) Mineral grain tracking for an example grain over 168 leaching days.

relatively evenly and there is no discernible trend in the extraction with horizontal position in the column (reflected by the weak linear correlation coefficient (r) and coefficient of determination (r^2)).

The lack of variation in extraction with height in the column or with horizontal position means that the variability between particles is virtually all due to local effects such as differences in the mineralogy of the particles and the spatial and size distribution of the grains within them.

The ore particle size effect is known to be an important mechanism affecting the sulphide dissolution (Ghorbani et al., 2011a), but the investigation of this dependency was not the aim of these experiments and a

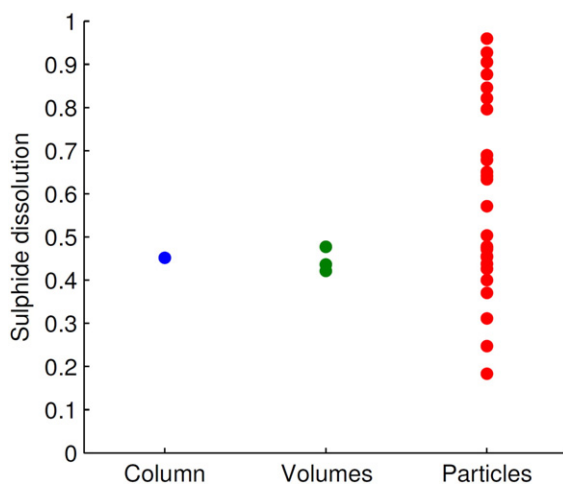


Fig. 3. Plot of the average sulphide dissolution for the entire column, the average sulphide dissolution for the three scanned volumes (top, middle and bottom) within the column and the sulphide dissolution for the individual ore particles.

narrow size distribution for the particles was deliberately chosen to try and limit this effect. Fig. 6 shows the sulphide dissolution against the initial ore particle size for all the tracked particles within the column. The total volume (in voxels) of each particle was measured using the voxel counting algorithm and converted into an equivalent spherical diameter (in mm). The narrow size distribution means that the particle to particle variability masks any underlying trend in extraction with size.

The three main sources of leach variability within the particles are likely to come from the size distribution of the grains, the variability in the inherent surface kinetics (mainly a function of mineralogy and mineral associations) and the distribution of the distances of the grains to the ore particle surface (which will impact the mass transfer rate). The mineral grain distance distribution can be measured and quantified by applying a 3D distance map. In the distance map analysis, each voxel is assigned a value depending on the distance to the nearest ore particle boundary. The boundary voxels of the object are assigned a value of zero whereas the assigned value increases as the distance from the boundary increases. Generally, the mineral grains closer to surface should leach faster than the minerals located in the centre of ore particle. This is because the shorter the distance to the surface, the easier it is for the leaching solution to diffuse in and the dissolved species to diffuse out. Fig. 7 shows a distance plot of an example particle over 168 days of leaching. A strong distance dependency can be observed.

Among all 26 particles, the majority have similar trends to that shown in Fig. 7, though there is still quite a bit of variability brought about by differences in the size and spatial distribution of the grains, as well as in their mineralogy. While there is likely to be little correlation on average, within individual particles grain size can be correlated with distance to the particle surface. In particular, the location and leach behaviour of a few large grains can have a disproportionate impact on these curves for an individual ore particle. Fig. 8 shows the average extraction with distance over all 26 of the measured particles after

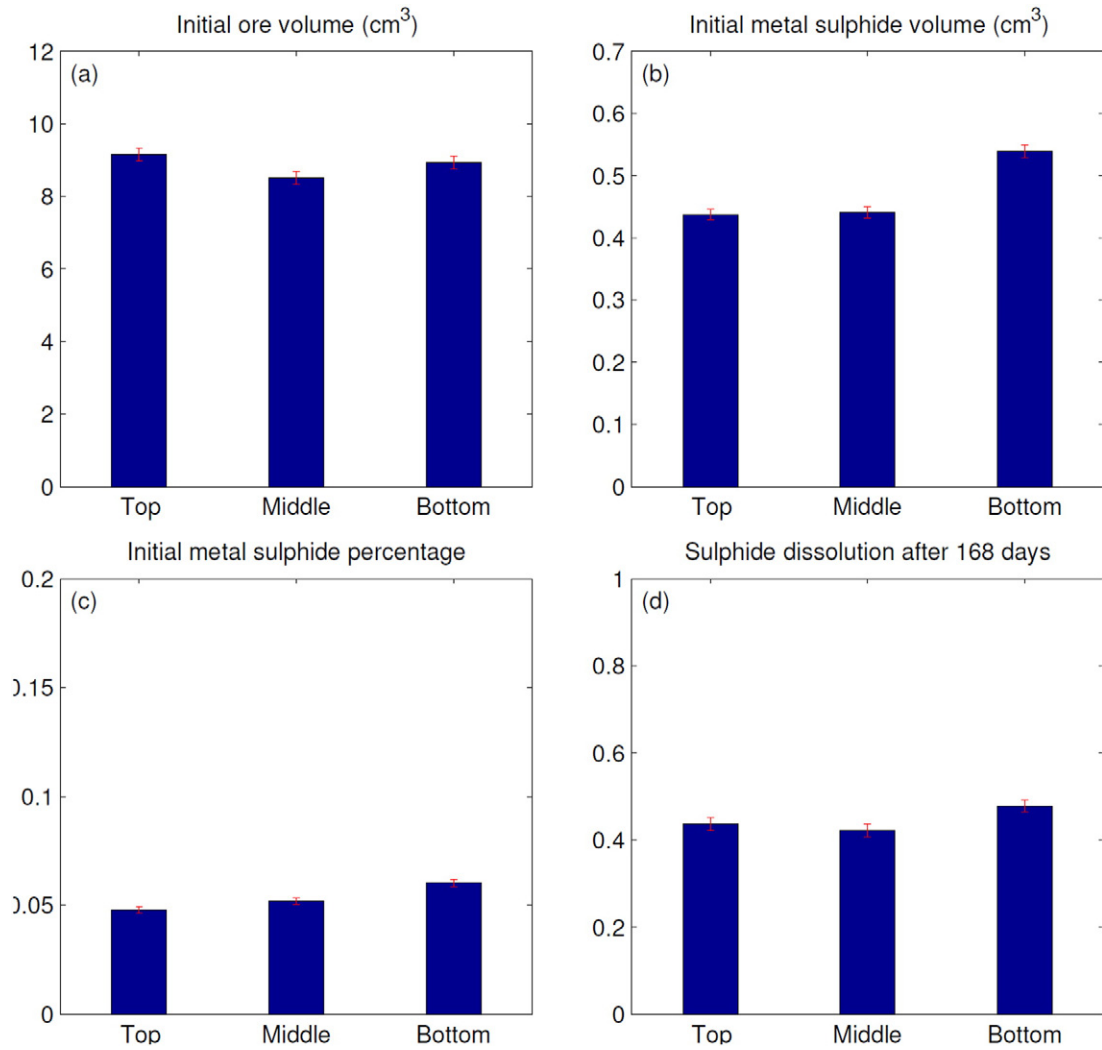


Fig. 4. The initial conditions of scanned volumes and their overall sulphide dissolution. The error bars indicate the uncertainty caused by the thresholding algorithm, which is $\pm 2\%$. The resolution of the scanning is approximately $17\ \mu\text{m}$. The value of $\pm 2\%$ is measured by comparing the total volume of tracked mineral grains for a rescanned volume to its reference volume (details shown in (Lin et al., 2015)). This error value is suitable for measuring the total volume of mineral grains with a wide size distribution rather than grains at a specific size.

168 days of leaching, as well as the extraction against distance curves for all 26 individual particles. To better understand these trends we need to decouple the effect of distance from that of particle size, though

fortunately the ability to track the leach behaviour of every single mineral grain means that we have a vast amount of data with which to do this (136,443 individual grains were tracked within the 26 particles).

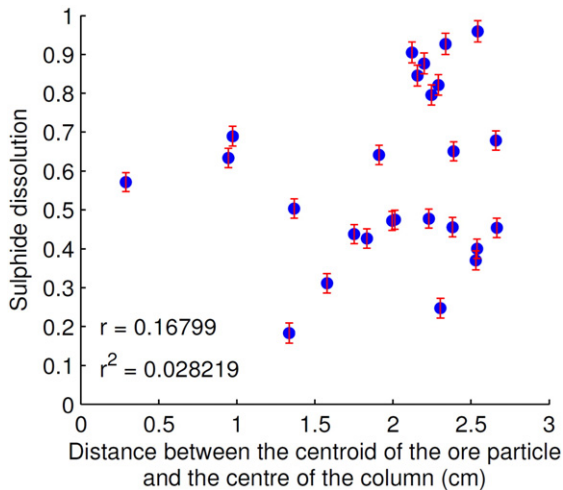


Fig. 5. The sulphide dissolution for all the tracked ore particles against the distance between the centroid of the ore particle and the centre of the column (pixels).

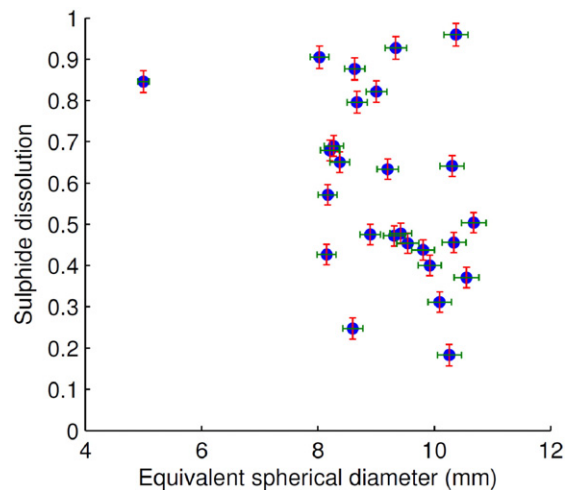


Fig. 6. The sulphide dissolution for all the tracked ore particles against their initial ore particle sizes.

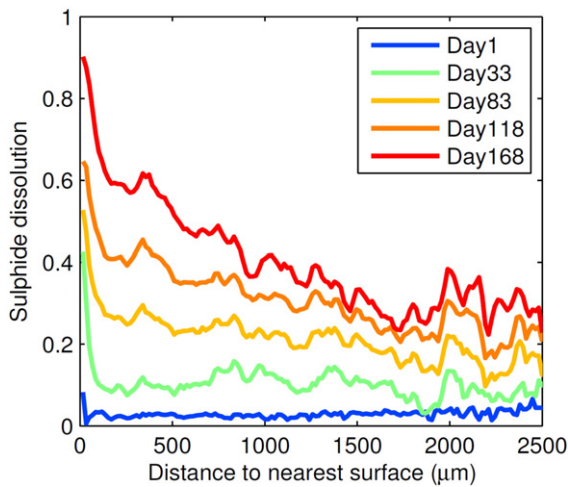


Fig. 7. Distance plot for an example ore particle over the 168 day leaching period.

4.2. Leach performance and its variability at the mineral grain scale

The mineral extraction is a strong function of its distance to the ore particle surface (see Fig. 8), though with quite a bit of variability between particles. Much of this leach variability is likely to be due to variability in the distributions of size and distance to the particle surface of the individual mineral grains. In order to fully understand the leach performance and its variability, and to determine the dominant mechanisms, the analysis thus needs to be carried out at the grain scale.

Analysing tens of thousands of grains individually is not very meaningful or efficient, especially for smaller grains, which have high measurement errors and uncertainties when considered on their own. Combining the measurements from many similar grains will, however, significantly reduce this uncertainty (Lin et al., 2015). Therefore, it is more useful to divide all the grains into different size–distance categories and study the average leach behaviour and its variability for each category. The grains were divided into categories based on size and distance to the surface with intervals chosen to give a reasonable distribution of the grains over the categories (see Fig. 9). Without having different size intervals for different distance categories it is impossible to perfectly balance the number of grains in each category. As they have smaller measurement errors associated with them, it is less

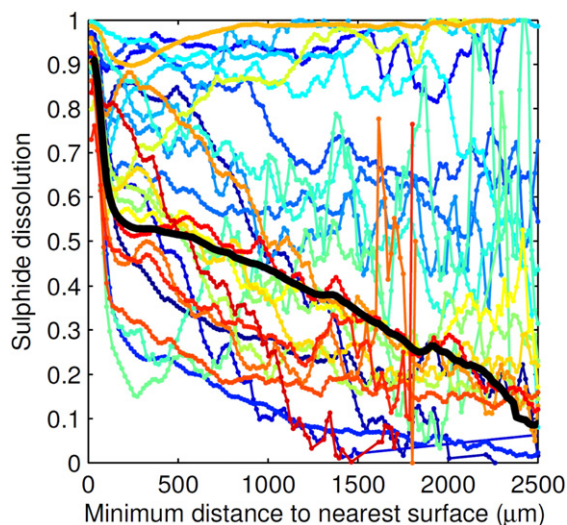


Fig. 8. Average sulphide dissolution for all tracked ore particles versus the distance between each grain and nearest surface over 168 leaching days.

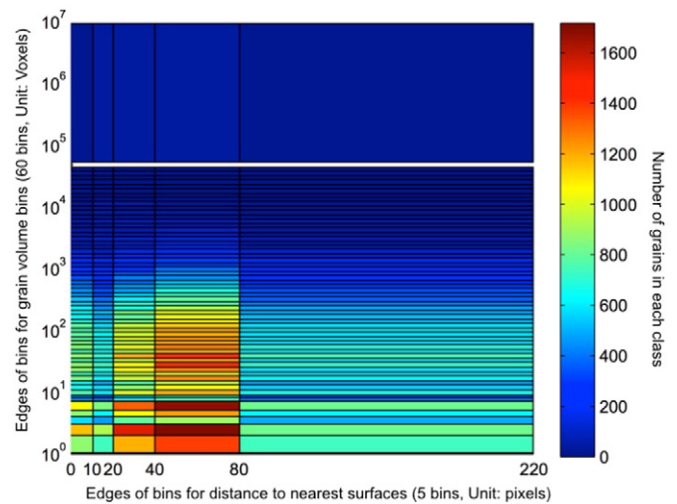


Fig. 9. Dividing tracked grain into different categories according to size and distance to surface. The colour indicates the number of grains in each category.

important to have a large number of grains in the categories with larger grain sizes (Lin et al., 2015).

The average sulphide dissolution for different size–distance categories is shown in Fig. 10. The categories shown are those with an average size larger than 100 voxels and a sample size larger than 10. A clear colour gradient can be observed with increasing average initial grain size and average distance to the ore surface. The colour gradient indicates that the grains with smaller size and shorter distance have higher leaching kinetics, as expected.

While it is obvious that the leach rate of a grain should depend upon its distance from the surface and its size, it is interesting to investigate the relative importance of these dependencies and how they vary with time. From Fig. 11 it can be seen that in all size and distance categories there is an initial rapid jump in the sulphide dissolution over the first few days of leaching. This is probably due to the small amount of oxides and secondary sulphides within the system (see Table 1), which are known to have much faster leach kinetics than the primary sulphides.

From Figs. 11 and 12 it can be seen that the size dependency is the dominant effect at short times, while the distance dependency becomes stronger at longer times. This change in relative importance of size and distance is probably not due to any change in the mechanisms involved, but is rather due to variability in the leach rates of the individual grains within a size and distance category. The extraction is being characterised by means of the initial size of the grains, which means that as time progresses the variability of the current size of the grains within a category becomes wider and thus the dependency on the initial size becomes weaker. The variability in the leach rate of grains within a size and distance category is likely to be mainly due to variability in the surface kinetics and thus a function of the variability in the mineralogy and its associations. It is thus important to investigate this variability in the leach rate within each category as it will have a major bearing on the apparent leach kinetics and their evolution with time.

Within a single ore particle, Fig. 13 shows the change in sulphide dissolution for 25 mineral grains chosen randomly out of those that have an initial volume of between 500 and 1000 voxels (this corresponds to initial equivalent spherical diameters of between about 75 µm and 95 µm). As well as these 25 randomly chosen grains, the average behaviour of all 394 mineral grains within this category is plotted. While the uncertainty in the size of the individual grains due to measurement error within this size range is small, it is not trivial (a relative standard deviation of about 3% to 4%), the effect of measurement error on the calculation of the average leach behaviour is tiny, though, due to the large

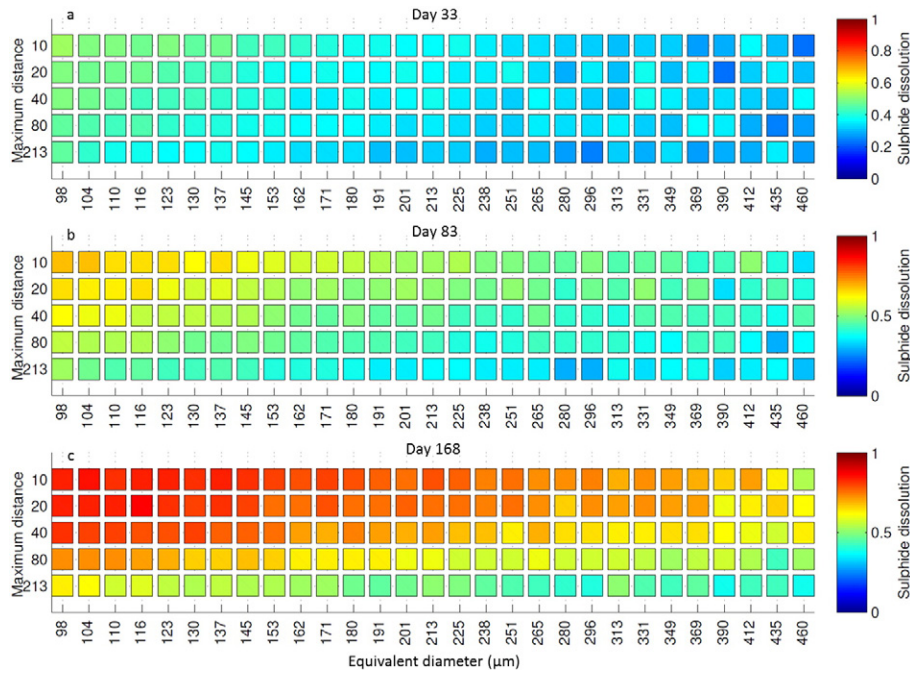


Fig. 10. Plots of average sulphide dissolution in each size–distance category in three difference time points using a colour map based on percentage dissolution: a) Day 33 b) Day 83 c) Day 186.

sample size (see Lin et al. (2015) for details on how the measurement uncertainty is obtained). The measurement uncertainty will be the reason why a small number of the recoveries for individual mineral grains are below zero, especially as these values are particularly sensitive to errors in the measured volume of the grains in the initial scan as this influences every subsequent dissolution value.

Our error analysis has shown that for all but the smallest grains (those below about 100 voxels (equivalent spherical diameter of ~98 µm with pixel size of 17 µm) the variability in the measured extraction is primarily due to variability in the actual underlying leach rate rather than measurement error. The error bars in Fig. 14 thus represent differences in the actual leach rate of grains, which have similar initial sizes and distances to the surface. This variability is likely to come from differences in the mineralogy of the grains themselves, as well as due to different mineral associations and local differences in the permeability of the rock surrounding the grains.

This variability in leach rate initially causes the variability in extraction to increase with time, but as the number of completely leached grains increases, the variability in the extraction starts to decrease again as, irrespective of the variability in the rate at which they are leached, fully leached grains have no variability in their extraction.

It is desirable to go a step further than simply looking at the variability in the extraction to look at the underlying grain scale variability in the leach kinetics as this can be used to estimate how the apparent leach kinetics are likely to vary with time and the macroscopic extent of extraction.

5. Estimating variability in the surface kinetics

The variability in the surface kinetics is an important factor in the ultimate performance of a heap as it controls how the apparent kinetics will evolve with time. Since grains with high leach kinetics will disappear faster than those with slow surface kinetics, the average surface kinetics will decrease with time. Additionally, the faster leaching classes such as grains near the particle surface or smaller grains will also disappear faster. The evolution of the apparent leach kinetics of a particle is thus the result of a complex interaction between the evolution of the surface rate kinetic distribution, the size and location distribution of

the grains and how these interact with mass transport within the particle. Accounting for all these factors is complex and can only really be assessed using a fully coupled modelling and simulation approach (e.g. Lin et al. (2016)). In this section of the paper we will concentrate on assessing the distribution of apparent surface rate kinetics and how this impacts the evolution of the mineral grain size distribution.

In order to assess the distribution of the surface rate kinetics we need to be able to use the extraction of the individual grains to calculate their rate kinetics. To do this we start with a very generic rate equation for surface kinetics. In the derivation below we have made no assumption about the order of the reaction (in fact, for the purposes of this derivation we need not even assume that there is a power law dependency):

$$F = kC^n \tag{1}$$

where F is the mass flux out of the grain, k is the surface rate constant and n is the order of the reaction. In this derivation C is the time dependent concentration experienced by grains within a particular category. The rate of change in the mass of a grain is equal to the flux out of the grain times its surface area:

$$\frac{dM}{dt} = -kAC^n \tag{2}$$

where M is the mass of the grain, A is the surface area. The surface area of a grain is proportional to its volume raised to a power $2/3$, with a proportionality, α , that depends on its shape:

$$A = \alpha V^{2/3} \tag{3}$$

The mass of the grain is, in turn, related to its volume by its density, ρ :

$$M = \rho V \tag{4}$$

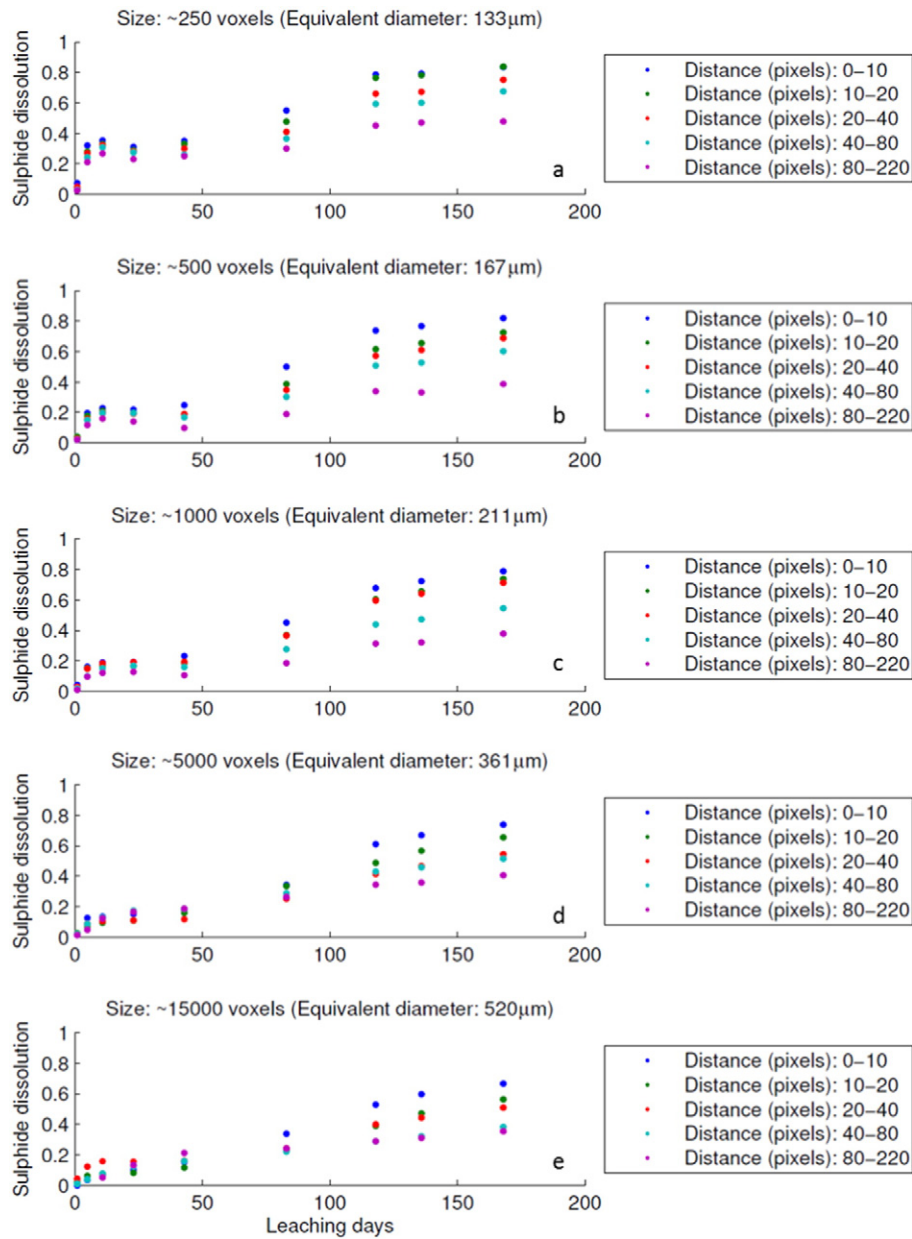


Fig. 11. The extent of dissolution (recovery) for categories with different average initial grain size at different distance against leaching time: a) ~250 voxels, b) ~500 voxels, c) ~1000 voxels, d) ~5000 voxels and e) ~15,000 voxels.

Combining these equations gives the following differential equation for the rate of change of grain volume:

$$\frac{dV}{dt} = -\frac{\alpha}{\rho} k V^{2/3} C^n \quad (5)$$

Eq. (5) can be integrated from the initial time to any subsequent time over which the grain volume changes from an initial volume, V_0 , to the volume at time t , V_t :

$$\int_{V_0}^{V_t} \frac{\rho}{\alpha V^{2/3}} dV = -k \int_0^t C^n dt \quad (6)$$

$$\frac{1}{3} (V_0^{1/3} - V_t^{1/3}) = \frac{\alpha}{\rho} k \int_0^t C^n dt \quad (7)$$

We can do the same analysis for the grain in the same size and distance category with the average surface rate, \bar{k} , for that category and a corresponding average volume after time t of \bar{V}_t :

$$\frac{1}{3} (V_0^{1/3} - \bar{V}_t^{1/3}) = \frac{\alpha}{\rho} \bar{k} \int_0^t C^n dt \quad (8)$$

In this analysis we are assuming that all the grains in a particular size and distance from the surface category experience the same concentration history. At a specific time, distance from the surface is thus treated as a proxy for concentration. This would be true if the permeability and initial grain distribution were uniform. Some of the variability in our apparent surface kinetics thus actually comes from mass transport variability. We do not need to assume that the concentration experienced by grains in a category remain constant with time, though, as that variability is included within the integral on the RHS of the above equations.

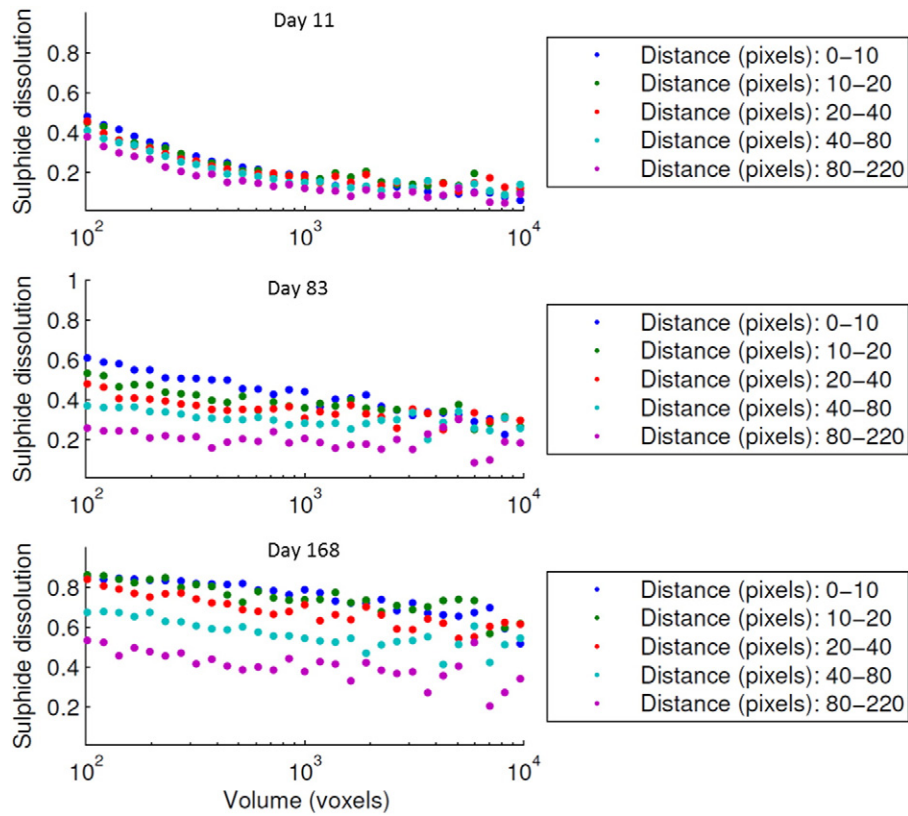


Fig. 12. The extent of dissolution (recovery) for different categories at different distance against average initial mineral grain size at different time points: e.g. Day 11, Day 83 and Day 168.

Dividing Eq. (7) by Eq. (8) removes all the dependencies other than that on the change in volume:

$$\frac{k}{\bar{k}} = \frac{\left(1 - \left(\frac{V_t}{V_0}\right)^{1/3}\right)}{\left(1 - \left(\frac{\bar{V}_t}{\bar{V}_0}\right)^{1/3}\right)} \quad (9)$$

This equation can also be written out in terms of the extraction from a grain ($R = 1 - \frac{V_t}{V_0}$):

$$\frac{k}{\bar{k}} = \frac{\left(1 - (1-R)^{1/3}\right)}{\left(1 - (1-\bar{R})^{1/3}\right)} \quad (10)$$

This analysis gives the surface rate constant of a grain relative to the average rate constant within a category and thus, by combining all the grains within a category, it can give the distribution of the apparent surface kinetics. In the analysis below, the distributions are calculated by using the sulphide dissolution of all the measured mineral grains over the first 23 days of leaching.

Fig. 15 shows the cumulative distribution of the relative rate constants for all the size and distance categories (i.e. based on all 136,443 grains). Even though the average leaching rates of the different categories were markedly different (see Fig. 10), the distributions of the relative rates are all remarkably similar.² This implies that this variability is predominantly a property of the mineral surfaces, local mineral

² In these distributions a few grains have negative apparent rates. This is probably because of measurement uncertainty in the change in volume for grains with little or no leach kinetics. The upward spikes to 1 in the distributions for some of the faster leaching categories are due to the time interval over which the analysis was conducted. In some of the fastest leaching categories a number of grains will be completely leached within the 23 day time interval used to produce this data, putting a limit on the maximum relative rate that can be measured.

associations and local mass transfer barriers, since more macroscopic variability effects would manifest themselves as changes in the shape of this distribution with distance from the mineral surface.

In Fig. 16 the average over all the distributions is plotted as a probability density function (PDF). This distribution has a major peak that is likely to be associated with the primary sulphides as these are both the slowest leaching and most abundant of the metal containing minerals. There is also evidence for smaller peaks in this distribution at much higher leaching rates. These peaks are most likely associated with oxides and secondary sulphides that are known to have much faster leach kinetics (Bartlett, 1998).

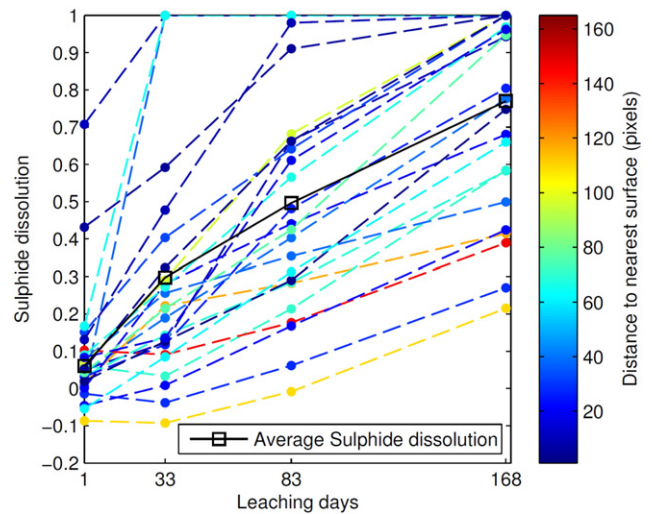


Fig. 13. The change in extent of dissolution (recovery) of 25 example grains with initial volumes of between 500 and 1000 voxels over the 168 days of leaching. In addition, the average dissolution behaviour for all 394 grains within this category is also plotted.

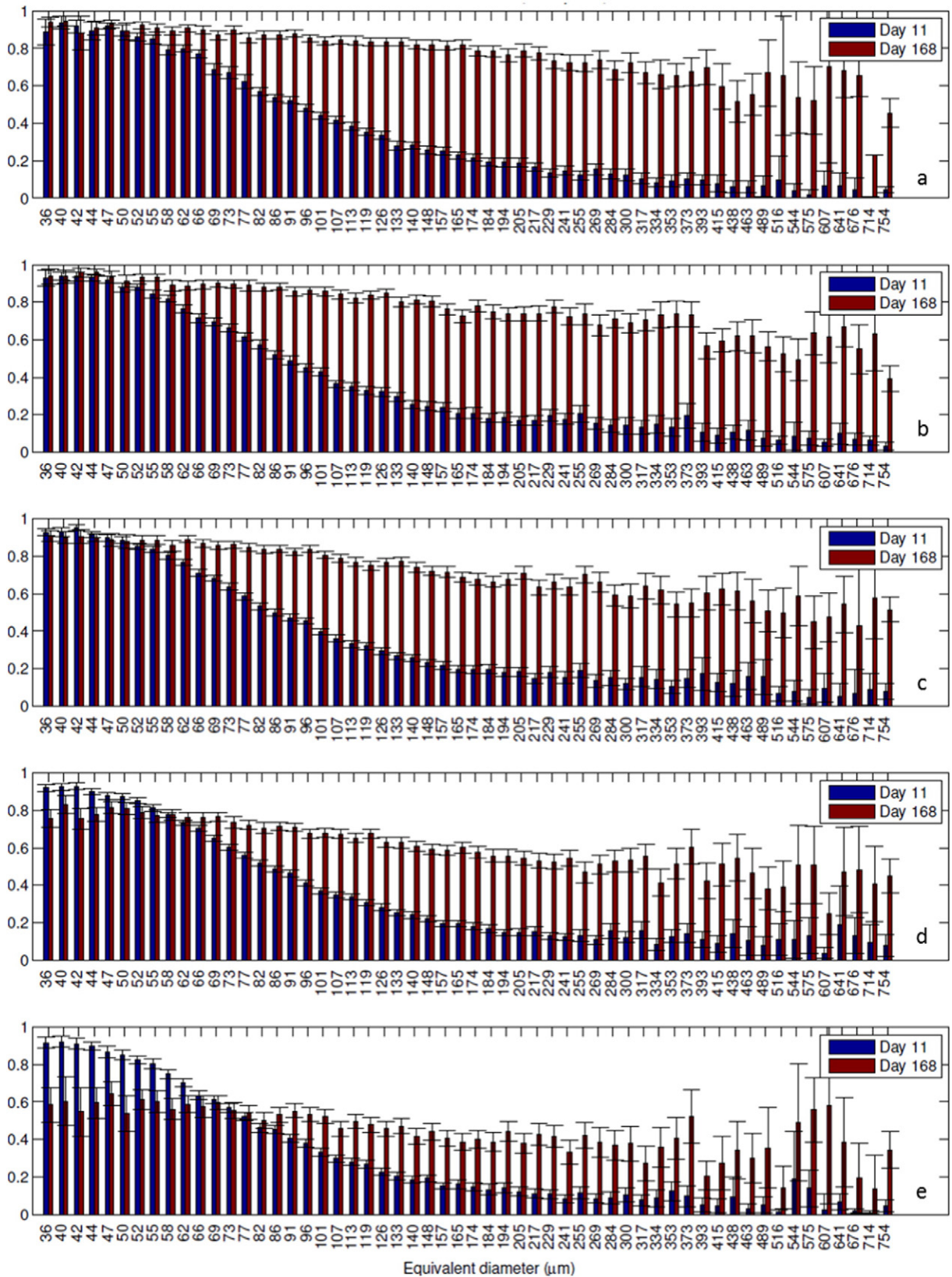


Fig. 14. The sulphide dissolution for all the size–distance categories with average initial grain size (equivalent spherical diameter) larger than 36 μm after Day 11 and Day 168. a) Distance 0–0.17 mm (0–10 pixels). b) Distance 0.17–0.34 mm (10–20 pixels). c) Distance 0.34–0.68 mm (20–40 pixels). d) Distance 0.68–1.36 mm (40–80 pixels). e) Distance 1.36–3.74 mm (80–220 pixels). The error bar measures the 95% confidence interval.

This underlying variability in the apparent surface leach kinetics together with the size and spatial distribution of the grains are key to the time evolution of the particle scale leach

kinetics. In a related paper (Lin et al., 2016) a methodology for incorporating this data into a detailed particle scale simulation is presented.

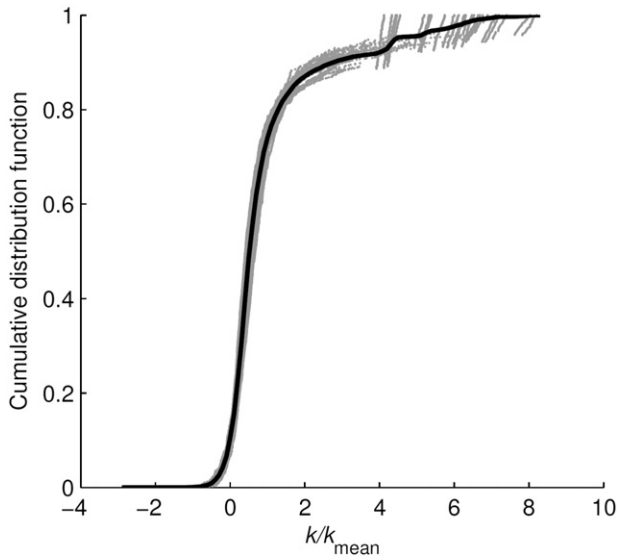


Fig. 15. Surface kinetics distribution for the leaching column. Cumulative distribution function of the relative rate constants for all the different size and distance categories (grey dots) and the average distribution function for all the categories (solid black line).

5.1. Calculating the evolution of the grain size distribution

The distribution of the surface kinetics (Fig. 16) can be used to calculate the distribution of the extractions for the grains within a category given an average extraction for the category. This is, in effect, the reverse of the procedure used to calculate the distribution in the first place, though it can be used for any average extraction, not just the measured ones.

The extraction within a size and distance category is a function time, though not a known function for an arbitrary category. The extraction for the grain with the average surface kinetics can thus be written as a function of a time dependent variable, T , with the form being chosen to make the subsequent analysis easier (note that the average extraction and the extraction for the grain with the average surface kinetics is not the same thing as the extraction rate for a grain is also

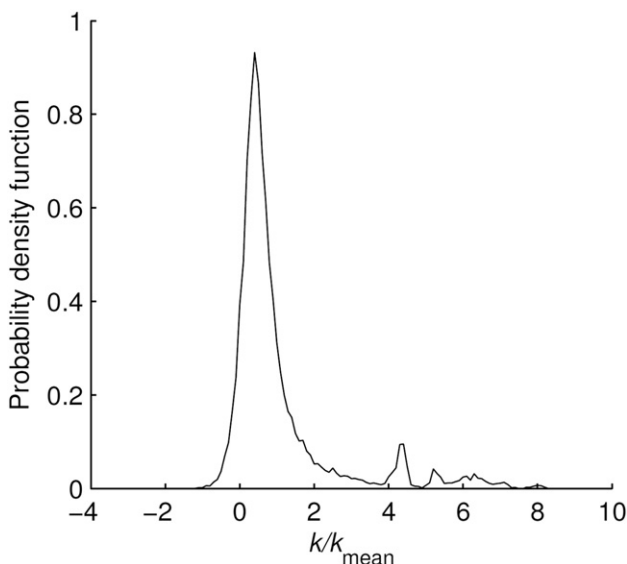


Fig. 16. Average data from Fig. 15 plotted as a probability density function (PDF).

proportional to its surface area, the distribution of which changes with time):

$$T = f(t) = 1 - (1 - \bar{R})^{1/3} \tag{11}$$

By combining Eqs. (10) and (11) and rearranging the following equation for the extraction of a grain with a specific relative rate constant, $\frac{k}{\bar{k}}$, is obtained. The reason for the inequalities in this equation is that extraction for a particular grain cannot be greater than 1.

$$R = \begin{cases} 1 - \left(1 - T \frac{k}{\bar{k}}\right)^3, & 1 - \left(1 - T \frac{k}{\bar{k}}\right)^3 \leq 1 \\ 1, & 1 - \left(1 - T \frac{k}{\bar{k}}\right)^3 > 1 \end{cases} \tag{12}$$

If $V_{initial}$ is the probability density function (Fig. 16) for the initial volume of grains with a relative surface rate constant k/\bar{k} (where $\int_0^\infty V_{initial} d\left(\frac{k}{\bar{k}}\right) = 1$), then the average extraction within a category after a specific time, R_{ave} , can be calculated:

$$R_{ave} = 1 - \int_0^\infty V_{initial} (1 - R) d\left(\frac{k}{\bar{k}}\right) \tag{13}$$

where R is a function of $\frac{k}{\bar{k}}$ (and T) as calculated from Eq. (12). Eq. (13) is complex to solve analytically for an arbitrary probability density function. In this paper this equation is solved numerically using the following approximation:

$$R_{ave} \approx 1 - \sum_{i=0}^N V_{initial,i} (1 - R_i) \Delta\left(\frac{k}{\bar{k}}\right)_i \tag{14}$$

where i is an interval in the value of $\frac{k}{\bar{k}}$ in the discrete version of the probability density function. This means that the distribution of recoveries (or, equivalently, sizes relative to the initial size) can be calculated as a function of the average extraction (see Fig. 17).³ In this calculation a value of T is chosen to given the desired value for the average extraction in a category by using Eq. (14) combined with an appropriate root finding algorithm (e.g. the “solve” function in Excel). As part of the calculation of Eq. (14), all the individual recoveries are calculated using Eq. (12).

It should be noted that this is not a calculation for the evolution of the grain size distribution within an overall ore particle, but is rather a calculation of the evolution of the grain size distribution for grains at a similar distance to the surface and similar initial size. The overall grain size distribution requires that the extraction in each category at the desired leach time, as well as the initial number of grains in that category, be known (see Figs. 9 and 10).

In Fig. 17 completely leached grains are included in the distribution, with a proportion indicated by the intercept on the y axis. The cumulative distribution function also goes vertically to 1 from about 0.95 at a relative grain volume of 1 due to the approximately 5% of grains that are unleachable. The experimental data that was used to validate these size distribution predictions were the size and distance categories at time points later than 80 days that had an average extraction closest to the 25%, 50% and 75% for which predictions were made (see Fig. 17 caption for details of the categories that most closely match these average extractions). Categories with a grain volume less than 100 voxels were not considered as the measurement error in these categories would be a significant portion of the variability for these grains

³ Note that in this calculation it is assumed that those grains with a negative rate have that rate due to measurement error and are therefore assigned a rate of zero.

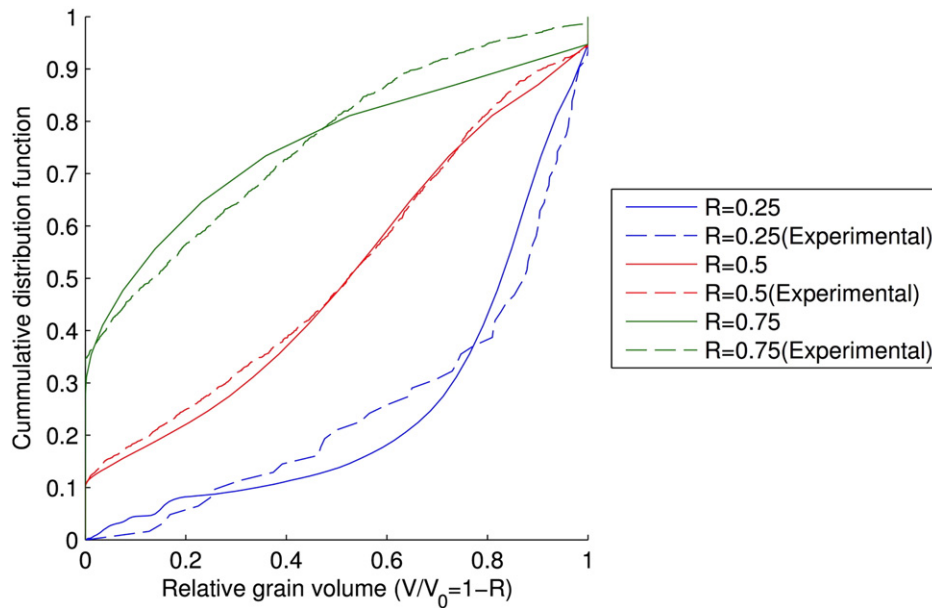


Fig. 17. Predicted distribution of mineral grain sizes within a narrow size and distance to the particle surface category after average extractions within the categories of 0.25, 0.5 and 0.75. The experimental size distributions are from the size and distance category at a particular time point that most closely matches the average extractions (Experimental: $R = 0.25$: Day 83–0.68 to 1.36 mm from surface – +400–438 μm diameter; $R = 0.5$: Day 83–0 to 0.17 mm from surface – +140–165 μm diameter; $R = 0.75$: Day 118–0 to 0.17 mm from surface – +125–140 μm diameter).

(measurement uncertainty is a strong function of grain size, with the measurement error only dropping below 5% of the volume for grains bigger than about 100 voxels, with this error continuing to drop rapidly with increasing grain size (Lin et al., 2015)). The reason for only considering time points beyond 80 days was that the kinetic variability was measured using experimental data over the first 23 days and we therefore wished to validate the grain size distribution predictions using data well beyond that used to make the predictions. It can be seen from the figure that even though each of the categories used involve very different sized grains, different distances to the surface and/or different leaching times, there is very good agreement between the prediction and the corresponding experiments.

Because of the variability in the surface leach rates, a particle's size and location does not completely dictate its evolution. At low recoveries the concave nature of the curve indicates that the average extent of dissolution is dominated by the rapid dissolution of relatively few fast leaching grains. As the overall extent of extraction increases the proportion of the grains contributing significantly to the dissolution needs to increase, while the faster leaching grains will have completely leached by this stage and therefore not contribute to any increase in the extraction. This means that the average surface kinetics of the grains will decrease with time. To some extent this will be countered by the fact that the grains near the surface will become depleted and thus reduce the mass transfer barrier for the grains deeper in ore particle (near surface grains will consume reagents before than can reach the deeper grains and will also release leached material and thus reduce the concentration gradients required for diffusive mass transport deeper in the particle).

Most of the surface kinetic variability will come from differences in the mineralogy of the grains and their associations (though some will also come from variability in the permeability of the material surrounding the grains). Ideally we would have liked to be able to associate the changes in the surface leach kinetics with the mineralogy, but unfortunately the x-ray attenuation of the sulphides in this system are virtually identical. At lower x-ray energies the attenuation contrast between the sulphides would increase, but while lower energies could be used for smaller samples, they could not be used on the comparatively large columns used in this study with a reasonable scan time. An alternative is to section a representative sample of particles post leaching and directly

determine their mineralogy. Unfortunately by the end of the leach period a large portion of the grains had completely dissolved and most of the remaining grains were pyrite, giving little insight into how the surface leach kinetic distribution correlated to the mineralogy.

6. Conclusions

In this paper tomographic quantification and multi-scale analysis was performed on a small scale leaching column over 168 leaching days. A huge variation (18%–96%) was found in the extents of extraction among the ore particles. However, no correlation was found between sulphide dissolution and the particle's location within the column. The narrow size distribution used also meant that the particle to particle variability was much stronger than any trend with respect to the size of the particles in the column. This meant that virtually all the variability in the extent of sulphide dissolution was due to variations in the mineral grain size and spatial distributions within the particles, as well as the grain mineralogy. In order to assess this a grain tracking algorithm was developed that allowed all the hundreds of thousands of mineral grains to be tracked in time as they underwent dissolution.

The massive data set produced meant that the grains could be binned into narrow size and distance to surface categories with enough grains in each category to not only assess changes in the average behaviour, but also the variability in this behaviour at the grain scale. It was found that, not unsurprisingly, the smaller grains leach quicker than larger ones and that those near the surface leach quicker than those near the centre of the particle. What was interesting, though was that the dependency on the initial grain size decreased with time. This was not because the dependency on the current size decreased, but was rather because the dependency of the current size on the initial size became weaker with time. This was because there was quite a large variability in the leach rate even within each narrow size and distance to the surface category.

This variability is caused by variability in the surface kinetics of the individual grains, which, in turn, will be dependent on the mineralogy of the grains and the permeability of the material surrounding the grains. We developed an equation and methodology by which the distribution of the surface rate kinetics could be distinguished from that associated with the specific location and size of the grain. This distribution

of kinetics is crucial to the performance of a heap and how it evolves with time. If this distribution is wide then the average initial kinetics will have little bearing on the long term kinetics of the systems, with the extraction slowing markedly with time as the faster leaching species are depleted. On the other hand, a narrow distribution would indicate kinetics that would be less variable with time, though there will always be a decrease in the kinetics as the grains near the surface are depleted and thus the kinetics become more dependent on those grains deeper within the particles.

The variability in the leach rate with grain size and distance from the surface together with the variability within a particular size and distance category are key factors in the time evolution of the apparent particle scale leach kinetics. This is because the more variability there is in the leach behaviour of individual grains, the more the effective leach rate will change with time as the faster leaching grains are depleted. This paper gives a methodology for the quantitative assessment of this variability, which is the first step in the development and validation of improved particle scale leach kinetic models.

Acknowledgements

This study was performed in the Rio Tinto Centre for Advanced Mineral Recovery at Imperial College London, and at the Manchester X-ray Imaging Facility at Harwell, which was funded in part by the EPSRC platform grant (EP/I02249X/1). The underlying raw data is not shared online due to its huge size, but representative sample data is included in the figures. The authors gratefully acknowledge Rio Tinto for their financial support for this project.

References

- Bartlett, R.W., 1998. *Solution mining: leaching and fluid recovery of materials*. second ed. Gordon and Breach Science Publishers, Australia.
- Blair, D., Dufresne, E., 2008. *The Matlab particle tracking code repository*.
- Bouffard, S.C., West-Sells, P.G., 2009. Hydrodynamic behavior of heap leach piles: Influence of testing scale and material properties. *Hydrometallurgy* 98 (1–2), 136–142.
- Córdoba, E.M., Muñoz, J.A., Blázquez, M.L., González, F., Ballester, A., 2008. Leaching of chalcocopyrite with ferric ion. Part II: Effect of redox potential. *Hydrometallurgy* 93 (3–4), 88–96.
- Dixon, D.G., Petersen, J., 2003. Comprehensive modelling study of chalcocite column and heap bioleaching. In: Riveros, P.A., Dixon, D.G., Dreisinger, D.B., Menacho, J. (Eds.), *Copper 2003 – Hydrometallurgy of Copper (Book 2)*. CIM, Montreal, Canada, pp. 493–516.
- Ghorbani, Y., Becker, M., Mainza, A., Franzidis, J.-P., Petersen, J., 2011a. Large particle effects in chemical/biochemical heap leach processes – a review. *Miner. Eng.* 24 (11), 1172–1184.
- Ghorbani, Y., et al., 2011b. Use of X-ray computed tomography to investigate crack distribution and mineral dissemination in sphalerite ore particles. *Miner. Eng.* 24 (12), 1249–1257.
- Ghorbani, Y., et al., 2013. Investigation of particles with high crack density produced by HPGR and its effect on the redistribution of the particle size fraction in heaps. *Miner. Eng.* 43–44, 44–51.
- Habashi, F., 1999. *A Textbook of Hydrometallurgy*. Vol. xii. *Métallurgie Extractive Québec, Québec* (739 pp.).
- Hiroyoshi, N., Miki, H., Hirajima, T., Tsunekawa, M., 2001. Enhancement of chalcocopyrite leaching by ferrous ions in acidic ferric sulfate solutions. *Hydrometallurgy* 60 (3), 185–197.
- Jergensen, G.V., 1999. Copper leaching, solvent extraction, and electrowinning technology. *SME*.
- Kappes, D.W., 2005. Heap leaching of gold and silver ores. In: Mike, D.A., Wills, B.A. (Eds.), *Developments in Mineral Processing*. Elsevier, pp. 456–478.
- Kapur, J.N., Sahoo, P.K., Wong, A.K.C., 1985. A new method for gray-level picture thresholding using the entropy of the histogram. *Comput. Vis. Graphics. Image Process.* 29 (3), 273–285.
- Ketcham, R.A., Carlson, W.D., 2001. Acquisition, optimization and interpretation of X-ray computed tomographic imagery: applications to the geosciences. *Comput. Geosci.* 27 (4), 381–400.
- Lin, Q., Neethling, S.J., Dobson, K.J., Courtois, L., Lee, P.D., 2015. Quantifying and minimising systematic and random errors in X-ray micro-tomography based volume measurements. *Comput. Geosci. UK* 77, 1–7.
- Lin, Q., Barker, D., Dobson, K., Lee, P.D., Neethling, S.J., 2016. Modelling particle scale leach kinetics based on X-ray computed micro-tomography images. *Hydrometallurgy*.
- Otsu, N., 1979. A threshold selection method from gray-level histograms. *IEEE Trans. Syst. Man Cybern.* 9 (1), 62–66.
- van Hille, R.P., van Zyl, A.W., Spurr, N.R.L., Harrison, S.T.L., 2010. Investigating heap bioleaching: Effect of feed iron concentration on bioleaching performance. *Miner. Eng.* 23 (6), 518–525.